An alternative approach for investigation of the wave-induced scour around pipelines

M. H. Kazeminezhad, A. Etemad-Shahidi and A. Yeganeh Bakhtiary

ABSTRACT

Scour around submarine pipelines remains a largely complex and not yet fully understood problem. In this study, wave-induced scour around submarine pipelines was investigated. Since various physical processes occur during the development of a scour hole, the effects of each process were considered by employing several nondimensional parameters. To find the effective parameters on equilibrium scour depth, the correlation between independent parameters (e.g. Keulegan–Carpenter number) and dependent parameter (nondimensional scour depth) were determined using different experimental data. Then, an Artificial Neural Network (ANNs) approach was used to develop a more accurate model for prediction of wave-induced scour depth around submarine pipelines. ANN models with different input parameters including gap to diameter ratio, Keulegan–Carpenter number, pipe Reynolds number, Shields number, sediment Reynolds number and boundary layer Reynolds number were trained and evaluated to find the best predictor model. To develop the ANN models, both holdout and tenfold cross-validation methods were used. In addition, an existing empirical method was examined. Results show that the empirical method has a significant error in the prediction of scour depth for the cases with an initial gap between pipe and seabed. It is also indicated that the ANN models outperform the empirical method in terms of prediction capability.

Key words | artificial neural networks, backpropagation algorithm, empirical method, submarine pipelines, wave-induced scour

M. H. Kazeminezhad
A. Etemad-Shahidi (corresponding author)
A. Yeganeh Bakhtiary
College of Civil Engineering,
Iran University of Science and Technology,
PO Box 16765-163,
Tehran,
Iran
Tel.: +98 2173 913170
Fax: +98 2177 454053
E-mail: *etemad@iust.ac.ir*

NOMENCLATURE

The following symbols are used in this paper:

a	near-bed wave orbital amplitude
B	a function of gap to diameter ratio
D	pipe diameter
d_{50}	mean grain diameter
e	initial gap between pipe and seabed
e/D	gap to diameter ratio
f_w	friction coefficient
g	gravitational acceleration
k	pipe roughness
k^*	relative pipe roughness
k_s	equivalent sand roughness
k_s/a	relative bed roughness
KC	Keulegan–Carpenter number
m	a constant related to the bed material
N	number of observations
N^H	number of hidden layer neurons
N^I	number of inputs
N^{TR}	number of training samples
O_i	observed value
P_i	predicted value
Re	pipe Reynolds number
Re_0	boundary layer Reynolds number
Re_s	sediment Reynolds number

doi: 10.2166/hydro.2010.042

S	equilibrium scour depth
SI	scatter index
S/D	nondimensional scour depth
T	wave period
U_m	maximum value of the undisturbed orbital velocity of water particles at the bed
u_{*w}	wave friction velocity
x_i	dependent parameter
y_i	independent parameter
z_0	zero level for velocity
δ	wave boundary layer thickness
μ	fluid dynamic viscosity
ρ	fluid density
ρ_s	sediment density
θ	Shields parameter
ω	wave angular frequency

INTRODUCTION

Utilization of submarine pipelines is an efficient way for the transportation of crude oil and gas continuously from offshore to onshore areas. Following the installation of pipelines on the seabed, the flow pattern around it will change due to the presence of the pipe. Variations of flow pattern around the pipe result in the formation of different vortices and turbulence generation in its vicinity (Sumer *et al.* 1991). These variations cause an increase in the bed shear stress and subsequently bring about an increase in the local sediment transport capacity. Therefore, if the pipelines lay on an erodible seabed it may face local scouring, leading to the free-spanning of pipelines. The scour process will continue until the scour reaches such a level that the bed shear stress around the pipeline becomes of the order of 1 of the bed shear stress for the undisturbed flow. At this level, the depth of the generated pit under the pipeline is called the equilibrium scour depth (Sumer & Fredsoe 2002). Scouring and creation of free-spanning may cause failure of pipelines.

Local scouring around submarine pipelines is very complex due to the fact that it is the result of different physical processes which arise from the fluid–structure–seabed interaction (Zhao & Fernando 2007). Hence it can be influenced by many environmental parameters such as flow, soil, etc. In the marine environment, the scour around pipelines arises from the action of the steady current and wave on the seabed. It may be classified into two categories: the clear water and the live bed scour (Sumer & Fredsoe 2002). In the former case, no sediment transport motion takes place far from the structure, while in the latter case, the sediment transport prevails over the entire bed.

In the last few decades several experimental studies have been performed to explore how scour takes place around submarine pipelines and how it can be predicted. Most of the previous experimental studies have been constrained to the scour under steady current (e.g. Mao 1986; Sumer *et al.* 2001). In comparison with the current-induced scour, fewer studies were reported on wave-induced local scour around pipelines. Lucassen (1984), Sumer & Fredsoe (1990), Cevik & Yuksel (1999), Pu *et al.* (2001) and Mousavi *et al.* (2006) have experimentally investigated the scour under wave action in the live bed condition. (Hereafter, Sumer & Fredsoe (1990), Pu *et al.* (2001) and Mousavi *et al.* (2006) are referred to as SF90, Pe01 and Me06, respectively). According to these studies, different relationships have been developed to estimate the equilibrium wave-induced scour depth based on the Keulegan–Carpenter number (KC) and gap to diameter ratio (e/D) in live bed conditions.

Numerical simulation of wave-induced scour around a pipeline is very complex and time-consuming; hence this kind of study is still very limited (e.g. Liang & Cheng 2005). Numerical models were mostly developed to simulate the current-induced scour around pipelines.

In recent years, soft computing tools (e.g. Artificial Neural Networks (ANNs) and Fuzzy Inference Systems (FIS)) have been used to simulate several complicated engineering problems. ANNs are known as flexible modeling tools with capabilities of learning the mathematical mapping between input and output variables of nonlinear systems. FIS is based on expertise expressed in terms of "IF–THEN" rules which can be used to predict uncertain systems. In recent years, ANNs and FISs have been used to predict the equilibrium scour depth around piles (Kambekar & Deo 2003; Bateni & Jeng 2007; Bateni *et al.* 2007*a*,*b*) and at culvert outlets (Liriano & Day 2001). These techniques have also been used in other fields of marine and coastal engineering such as nearshore process and

coastal modeling (Ruessink 2005; Chau 2006), wind–wave prediction (e.g. Deo *et al.* 2001; Kazeminezhad *et al.* 2005; Zhang *et al.* 2006; Mahjoubi *et al.* 2008) and ecological system analysis in coastal waters (Muttil & Chau 2006; Chau & Muttil 2007).

Since the scour is a result of different physical processes, it is necessary to investigate the effects of each process by considering the relevant nondimensional parameters, whereas the proposed methods in the literature are all based on KC and e/D. Moreover, the soft computing models have not been developed as an appropriate predictor model for estimation of wave-induced scour depth. Therefore, the main objectives of this study are to identify the important parameters that affect the equilibrium scour depth and to develop a suitable ANN-based model for accurate prediction of the equilibrium wave-induced scour depth below submarine pipelines. To do so, the experimental datasets of SF90, Pe01 and Me06 are used. First, a correlation-based sensitivity analysis is performed to identify the governing nondimensional parameters. Then the accuracy of the proposed equation by Sumer & Fredsoe (2002), hereafter termed SF02, is examined. Finally, the ANN technique is used to find the effects of different nondimensional parameters on the scour depth and also to develop an ANN model (based on holdout and tenfold cross-validation methods) for the prediction of wave-induced scour depth around submarine pipelines. It should be noted that, in some previous applications of ANN, the holdout method has been used for limited data to develop an error estimate of the models. In this study the holdout and tenfold cross-validation methods are used for ANN modeling and the results are compared.

WAVE-INDUCED SCOUR AROUND SUBMARINE PIPELINE

The process of scour around pipelines laid on a mobile bed is rather complicated due to the occurrence of various physical processes arising from the triple interaction of fluid–sediment–structure. Figure 1 illustrates a submarine pipeline placed on the seabed and exposed to the wave in which D, e and a are the pipe diameter, initial gap between pipe and seabed and the near-bed

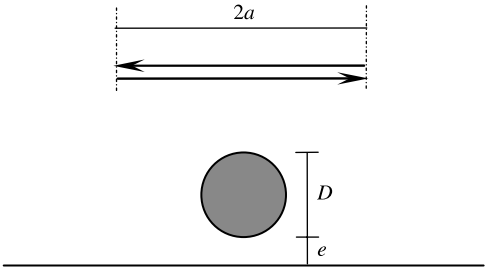

Figure 1 | Definition sketch of pipe placed near the seabed and exposed to wave/oscillatory flow.

wave orbital amplitude, respectively. It is seen that the wave is assumed as an oscillatory flow. Generally, wave-induced sediment transport is controlled by the oscillatory wave boundary layer. Therefore, in physical modeling of sediment transport, oscillatory flow is used instead of the wave (SF90).

Parameters involved

To investigate the wave-induced scour around a pipeline, the parameters identifying fluid, flow regimes, pipelines and bed material should be considered; hence the equilibrium scour depth around a pipeline can be described by the following functional relationship:

$$S = f(\rho, \mu, U_m, T, D, k, e, \rho_s, d_{50}, g) \tag{1}$$

where ρ is the fluid density, μ is the fluid dynamic viscosity, U_m is the maximum value of the undisturbed orbital velocity of water particles at the bed, T is the wave period, D is the pipe diameter, k is the pipe roughness, e is the initial gap between pipe and bed, ρ_s is the sediment density, d_{50} is the mean grain diameter, g is the gravitational acceleration and S is the equilibrium scour depth. In Equation (1), the effects of waves were considered by U_m and T parameters. In the nondimensional form, the equilibrium scour depth can be presented as follows (Sumer *et al.* 1991):

$$\frac{S}{D} = f\left(\frac{e}{D}, KC, Re, \theta, k^*\right) \tag{2}$$

in which $KC = U_m T/D = 2\pi a/D$ is the Keulegan–Carpenter number, $Re = \rho U_m D/\mu$ is the pipe Reynolds number, $k^* = k/D$ is the relative pipe roughness and θ is the Shields

parameter. The Shields parameter is calculated by the following equation:

$$\theta = \frac{u_{*w}^2}{((\rho_s/\rho) - 1)gd_{50}} \tag{3}$$

where u_{*w} is the wave friction velocity defined as (Van Rijn 1993)

$$u_{*w} = \sqrt{\frac{f_w}{2}} U_m \tag{4}$$

where $f_w = 1.39(a/z_0)^{-0.52}$ is the friction coefficient (Soulsby 1997), a is the near-bed wave orbital amplitude, $z_0 = k_s/30$ is the zero level for velocity and $k_s = 2.5d_{50}$ is the equivalent sand roughness (Van Rijn 1993). If the pipe's surface is hydraulically smooth, k^* is eliminated in Equation (2). An alternative approach is described later to select the effective parameters in wave-induced scour depth.

Existing empirical methods

Several experimental studies have been conducted to recognize the wave-induced scour around submarine pipelines and to propose an appropriate method to estimate the equilibrium wave-induced scour depth. SF90 investigated the mentioned phenomenon in wave flumes and also in U-shaped tubes. Their experiments were performed for the special conditions in which the sandy bed was plain, the live bed condition was dominating and the wave-induced flows were perpendicular to the pipe axis. They reported a weak influence of both the pipe Reynolds number and Shields parameter on the equilibrium scour depth in the live bed condition. SF02 presented the following equation for the prediction of S/D in live bed conditions, according to their experiments and the experiments of Lucassen (1984):

$$\frac{S}{D} = 0.1\sqrt{KC}\exp\left(-0.6\frac{e}{D}\right) \tag{5}$$

In accordance with the above equation, the wave-induced scour depth is influenced strongly by the Keulegan–Carpenter number and gap to diameter ratio parameter. Cevik & Yuksel (1999) proposed a formula to estimate the wave-induced scour around pipelines based on their experiments and those of the SF90 experiments. Referring to the SF90 study, they assumed that the effect of the Shields parameter on the scour depth is very weak and proposed the following formula for the live bed condition with no gap between pipe and seabed:

$$\frac{S}{D} = 0.11KC^{0.45}. \tag{6}$$

Pe01 also experimentally investigated the scour around submarine pipelines exposed to oscillatory flow motion. Their tests were carried out in the U-shaped tube and the main focuses were on the influence of bed material on the equilibrium scour depth. They proposed the following equation for S/D prediction around pipelines in the live bed condition:

$$\frac{S}{D} = B.KC^m. \tag{7}$$

where m is a constant related to the bed material (e.g. $m = 3.18$ for sandy bed) and B is a function of gap to diameter ratio (e/D), pipe diameter (D) and bed material.

Me06 also studied this subject in a wave flume and proposed the following equation for cases with small KC number in the live bed condition:

$$\frac{S-e}{D} = 0.1\sqrt{KC} \tag{8}$$

As seen, the proposed empirical methods are all based on the KC number and e/D.

ANALYSES

Dataset

The dataset used in this study comprises the SF90, Pe01 and Me06 experimental data. The SF90 experiments were carried out partly in a wave flume ($KC < 100$) and partly in an oscillatory U-shaped tube ($KC > 100$). Since for the marine pipelines exposed to the wind wave, the KC number is less than 100 (SF90), the experiments with KC number less than 100 were selected. The pipe surface acted as a hydraulically smooth surface and the

Table 1 | Full dataset

Data set	D (cm)	U_m (cm/s)	T (s)	d_{50} (cm)	e/D	S/D	Data set	D (cm)	U_m (cm/s)	T (s)	d_{50} (cm)	e/D	S/D
SF90	5	9.90	0.90	0.058	0	0.08	Me06	11	19.70	1.92	0.04	0.055	0.13
SF90	5	22.80	1.43	0.058	0	0.28	Me06	11	19.60	1.64	0.04	0.064	0.06
SF90	3	13.70	2.38	0.058	0	0.23	Me06	11	11.00	1.65	0.04	0.055	0.09
SF90	3	27.10	1.23	0.058	0	0.33	Me06	11	14.30	3.21	0.04	0.082	0.04
SF90	3	22.00	1.82	0.058	0	0.37	Me06	6	18.70	1.9	0.04	0	0.29
SF90	3	17.70	2.50	0.018	0	0.50	Me06	11	21.40	2.12	0.04	0.182	0.08
SF90	3	19.90	2.33	0.058	0	0.48	Pe01	2.89	15.29	2.59	0.02	0	0.26
SF90	3	18.40	3.70	0.058	0	0.52	Pe01	2.89	16.85	2.59	0.02	0	0.37
SF90	3	38.80	2.70	0.018	0	0.70	Pe01	2.89	15.18	2.59	0.02	0.290	0.17
SF90	3	27.06	1.22	0.018	0.260	0.34	Pe01	2.89	12.83	2.59	0.02	0	0.22
SF90	3	27.06	1.22	0.018	1.000	0.03	Pe01	2.89	16.96	2.59	0.02	0.690	0.20
SF90	3	25.70	3.13	0.058	1.030	0.22	Pe01	19.1	180.68	2.59	0.02	0	0.55
SF90	3	25.70	3.13	0.058	2.040	0.16	Pe01	19.1	153.39	2.59	0.02	0	0.41
SF90	3	20.90	2.70	0.058	0	0.67	Pe01	19.1	120.20	2.59	0.02	0	0.23
SF90	3	34.70	2.00	0.018	0	0.45	Pe01	19.1	110.62	2.59	0.02	0.490	0.02
SF90	3	25.70	3.13	0.058	0	0.70	Pe01	19.1	141.59	2.59	0.02	0.720	0.04
SF90	2	27.10	1.49	0.018	0	0.60	Pe01	19.1	171.09	2.59	0.02	0.490	0.21
SF90	1	26.50	3.13	0.058	0	1.00	Pe01	19.1	235.25	2.59	0.02	0.995	0.25
SF90	5	25.20	1.19	0.058	0	0.20	Pe01	19.1	171.09	2.59	0.02	0.720	0.22
SF90	3	24.00	4.55	0.058	0	0.70	Pe01	19.1	92.18	2.59	0.02	0	0.11
SF90	3	27.06	1.22	0.018	0.5	0.16	Pe01	19.1	166.66	2.59	0.02	0.490	0.19
SF90	3	27.06	1.22	0.018	0	0.47	Pe01	19.1	159.29	2.59	0.02	0.995	0.11
SF90	1	19.50	2.86	0.058	0	0.95	Pe01	19.1	142.33	2.6	0.02	0.49	0.09
SF90	1	14.70	2.86	0.018	0	0.60	Pe01	19.1	168.88	2.6	0.02	0.995	0.22
SF90	1	25.90	3.57	0.058	0	1.10	Pe01	19.1	134.22	2.6	0.02	0.995	0.03
Me06	11	17.30	1.40	0.04	0	0.21	Pe01	2.89	14.06	2.6	0.02	0	0.32
Me06	11	12.60	2.34	0.04	0.036	0.13	Pe01	2.89	15.62	2.6	0.02	0.69	0.11
Me06	11	23.30	1.37	0.04	0.027	0.0 9							

wave-induced current was perpendicular to the pipe in all experiments. Detailed information about the dataset is presented in Table 1. The other nondimensional parameters (e.g. *KC*, *Re*) were calculated based on the equations presented in the section on parameters involved. Table 2 summarizes the range of the nondimensional parameters in different experiments. As can be seen, SF90 experiments embrace a wide range of *KC*, while Me06 experiments are bound to the low *KC* values, where the interaction of wave–pipeline is weak. Pe01 experiments cover a wide range of *Re* numbers; thereby the order of the *Re* number is similar to that of the field.

Effective parameters

In this section the effective nondimensional parameters in the wave-induced scour around submarine pipelines are recognized by considering the involved physics. Due to the existence of various physical processes such as flow–seabed interaction, flow–structure interaction and sediment transport, the effects of each process should be considered to achieve an accurate scour model. The way that a pipe is installed on the seabed, how flow affects the pipe and seabed and characteristics of the generated boundary layer are the most important aspects of the wave-induced scour. When a smooth pipe lies on a plain bed the relevant nondimensional

Table 2 | Summary of test conditions in different experimental works

Data set	Reference	No. of data	Range of KC	$Re \times 10^3$	θ	Re_s	$Re_0 \times 10^3$
SF90	Sumer & Fredsoe (1990)	25	2–94	5–12.6	0.035–0.29	2.24–21.2	5.6–259
Pe01	Pu *et al.* (2001)	21	11–32	3.7–500	0.055–4.1	2.98–22.63	27–9,130
Me06	Mousavi *et al.* (2006)	9	1.5–6	11.2–25.6	0.04–0.136	6.32–11.55	12.7–61.8

parameters can be presented by the following relationship:

$$\frac{S}{D} = f\left(\frac{e}{D}, KC, Re, \theta, Re_s, Re_0, \frac{k_s}{a}\right) \tag{9}$$

These parameters are classified as follows: (i) the e/D parameter describing the position of the pipe in relation to the seabed; (ii) the KC and Re numbers describing the flow pattern around the pipelines; (iii) the sediment Reynolds number, $Re_s = \rho u_* d_{50}/\mu$ and θ depicting the mutual effects of flow on the seabed and (iv) the boundary layer characteristics represented by the boundary layer Reynolds number, $Re_0 = \rho U_m \delta/\mu$ and relative bed roughness, k_s/a, (Jonsson 1967) in which $\delta \approx (2\upsilon/\omega)^{0.5}$ and $\omega = 2\pi/T$ is the wave angular frequency. Another definition of boundary layer Reynolds number which was used in this study is $Re_0 = \rho U_m a/\mu$ (Jonsson 1967). The relative bed roughness concept is considered in the calculation of the friction coefficient (f_w) and Shields parameter. Therefore, the relative bed roughness can be eliminated in Equation (9). The concluding functional relationship for the equilibrium nondimensional wave-induced scour depth around submarine pipelines can be written as follows:

$$\frac{S}{D} = f\left(\frac{e}{D}, KC, Re, \theta, Re_s, Re_0\right). \tag{10}$$

In the above equation the KC number represents the formation and extension of the wake pattern in oscillatory motion and the Shields number represents the sediment transport mechanism.

Data analysis

As seen earlier, the proposed equations for the estimation of the equilibrium scour depth in the live bed condition depend mainly on KC and e/D. The effects of other parameters on the scour depth were assumed to be weak and negligible in the previous studies. Application of sensitivity analysis is essential to identify the effective parameters that affect S/D. To measure the association between the independent parameters introduced on the right-hand side of Equation (10) and S/D, correlation-based sensitivity measures were used in terms of the linear correlation coefficient (Manache & Melching 2008). The correlation coefficient was calculated as follows:

$$R = \frac{\sum_i (x_i - \bar{x})(y_i - \bar{y})}{\sqrt{\sum_i (x_i - \bar{x})^2 \sum_i (y_i - \bar{y})^2}} \tag{11}$$

in which x_i is the dependent parameter, y_i is the independent parameter and the overbar denotes the mean of parameters.

Table 3 shows the correlation coefficients between independent nondimensional parameters (e.g. KC, e/D) and nondimensional scour depth (S/D). It should be mentioned that the correlations were calculated between the logarithm of the dependent parameter and independent parameters. According to Table 3, the correlation coefficients between KC number and S/D in the SF90 dataset is 0.83, while in Pe01 and Me06 they are 0.22 and 0.39, respectively. It is also seen that e/D is correlated significantly with the equilibrium scour depth. Besides, there are considerable correlations between the other nondimensional parameters (e.g. Re, θ) and S/D in many cases. Therefore, the other nondimensional parameters which represent the mutual effects of flow on structure and seabed

Table 3 | Correlation coefficient between the nondimensional parameters and S/D in different experimental datasets

Dataset	KC	e/D	Re	θ	Re_s	Re_0
SF90	0.83	0.59	0.39	0.49	0.07	0.51
Pe01	0.22	0.54	0.23	0.39	0.19	0.19
Me06	0.39	0.78	0.32	0.41	0.22	0.14

and the boundary layer characteristics should be considered in estimation of the equilibrium scour depth. It is worth mentioning that most of the SF90 experiments were carried out with $e/D = 0$, while most of the Pe01 and Me06 experiments were conducted with $e/D > 0$. This difference may explain the difference between KC number and S/D correlations in these different datasets. To investigate this issue, the dataset was divided into two parts (data points with $e/D = 0$ and data points with $e/D > 0$) and the correlations between KC number and S/D were calculated for each part and shown in Table 4. It is readily seen that, as expected, for the cases with no initial gap ($e/D = 0$), the KC number is correlated significantly with S/D.

Regarding the above discussions, it is necessary to evaluate the accuracy of the empirical equations proposed for the estimation of S/D. Since the Me06 equation has been proposed for the low range of KC numbers and the Pe01 equation has been proposed for the specific pipe diameters, the SF02 equation which has been presented based on extensive experiments is evaluated using different experimental data.

Evaluation of the Sumer and Fredsoe equation

The comparison between measured and predicted nondimensional scour depth is shown in Figure 2. As can be seen, the SF02 equation overestimates S/D for the low values of S/D and underestimates it for high values of S/D.

For statistical comparison of predicted and measured nondimensional scour depth, bias and scatter index were used (SI):

$$\text{bias} = \frac{1}{N}\sum_{i=1}^{N}(P_i - O_i),$$
$$SI = \left(\sqrt{\frac{1}{N}\sum_{i=1}^{N}(P_i - O_i)^2}\right)\Big/\left(\sum_{i=1}^{N} O_i\right) \quad (12)$$

Table 4 | Correlation coefficient between the KC and S/D in different experimental datasets

e/D	No. of data	Correlation between KC and S/D
$= 0$	30	0.89
> 0	25	0.44

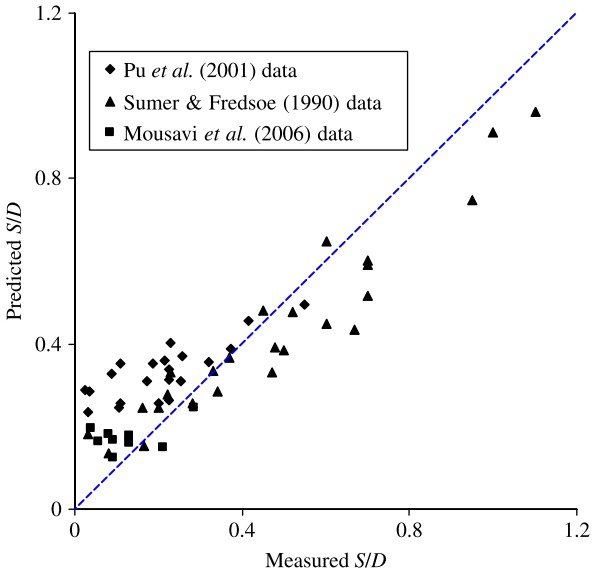

Figure 2 | Comparison between measured and predicted S/D by the SF02 equation.

where O_i is an observed value, P_i is a predicted value and N is the number of observations.

For a more comprehensive evaluation of the SF02 equation, the error statistics were presented separately for each dataset (Table 5). It is seen that the SF02 method slightly underestimates the S/D with a scatter index of 23.1% for the SF90 dataset. It is also evident that this equation is more appropriate for the cases with no initial gap between the pipe and seabed. The error statistics of calculated scour depth for the Pe01 and Me06 datasets

Table 5 | Error statistics of the predicted S/D by the SF02 equation for SF90, Pe01, Me06 and the full dataset

Dataset	e/D	No.	Average S/D	SI (%)	Bias
SF90	$= 0, > 0$	25	0.47	23.1	−0.044
	$= 0$	20	0.55	21	−0.067
	> 0	5	0.18	46.5	0.045
Pe01	$= 0, > 0$	21	0.21	73	0.12
	$= 0$	8	0.31	40.1	0.086
	> 0	13	0.14	114.9	0.149
Me06	$= 0, > 0$	9	0.12	66.9	0.05
	$= 0$	2	0.25	21.04	−0.051
	> 0	7	0.09	101.25	0.079
SF90, Pe01, Me06	$= 0, > 0$	55	0.32	39.26	0.036
	$= 0$	30	0.46	24.64	−0.025
	> 0	25	0.14	98.2	0.108

show that the SF02 equation is not accurate in the prediction of scour depth when there is an initial gap between the pipe and seabed. The overall statistical errors of the SF02 equation for all the datasets shows that it overestimates the scour depth (bias = 0.036) with a scatter index of 39.26%. Besides, this method is not accurate ($SI = 98.2\%$) in the prediction of S/D for the cases with $e/D > 0$, while it performs well ($SI = 24.64\%$) for the cases with $e/D = 0$.

As discussed before in addition to KC number and e/D, the other parameters should be considered for estimating S/D. Evaluation of the SF02 equation, which is based on the KC number and e/D, indicated that this equation is not very accurate in the prediction of equilibrium scour depth. Therefore, it is necessary to develop a wave-induced scour depth predictor model with all nondimensional parameters. To do so, the Artificial Neural Network (ANNs) concept which is described below is used.

MODEL DESIGN FOR PREDICTION OF S/D

Artificial neural networks (ANNs)

The development of artificial neural networks started in the early middle of the last century to help cognitive scientists in understanding the complexity of the nervous system (McCulloch & Pitts 1943). ANNs can be classified in terms of their topology (e.g. single- and multi-layer feedforward networks). The multi-layer feedforward networks have been applied extensively to solve various engineering problems in recent years (e.g. Kerh & Yee 2000; Azamathulla *et al.* 2008). Figure 3 displays the three-layer feedforward network. As can be seen the network is composed of three layers which are the input layer, with neurons representing the input fields, one hidden layer and an output layer, with a neuron representing the output field. Each neuron performs a weighted sum of its inputs and calculates an output using certain predefined transfer functions. Transfer functions for the hidden neurons are needed to introduce the nonlinearity into the network.

To train the network, it is fed with a set of input–output pairs called training data to reproduce the outputs. The training is done by adjusting the neuron weights and biases

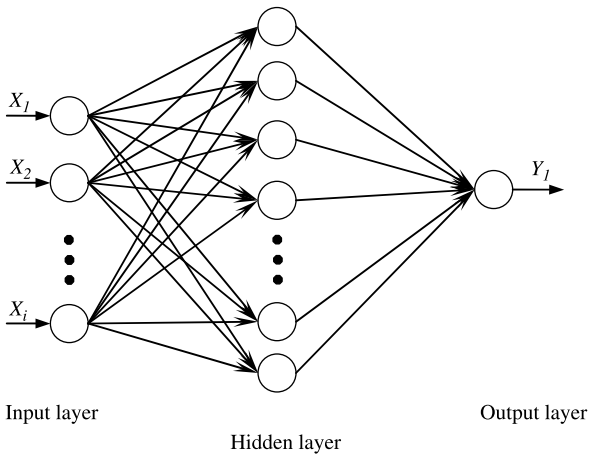

Figure 3 | Three-layer feedforward network.

using an optimization algorithm that attempts to minimize the differences between the network outputs and actual outputs. Backpropagation is one of the training techniques usually used for this purpose. After the training process, a new dataset called testing data is used to measure the generalization ability of the network and to know how accurately the network predicts outputs for inputs that are not used in the training data.

Finding the optimal number of hidden layers and neurons is an important step in the overall design of ANNs. Increasing the number of neurons in the hidden layer or adding more hidden layers to the network leads to low training error but network generalization degrades and overfitting is occurred (Geman *et al.* 1992). When new data (testing data) is presented to an overfitted network the error is large.

Data for ANN simulations

One of the most important stages in the design of an ANN model is the data collection and data preparation; thus the examples for training must be representative of all the possibilities concerning the application. In this study the dataset consisting of 55 data points was used to develop and validate the ANN-based predictor model for the prediction of S/D.

There are several methods for error estimation such as holdout and k-fold cross-validation (Stone 1974) methods. When the amount of data is large, the holdout method, which partitions all the data into two disjoint subsets

(training and testing sets), can be used. This method is used in the next section by dividing the dataset into two groups. The first one comprised of 42 data points is used as the training data and the second one comprised of 13 data points is used as the testing data. The percentage of the training and testing data is similar to that of Kambekar & Deo (2003).

In cases where the data is limited the k-fold cross-validation can be employed (Witten & Frank 2005). In k-fold cross-validation the data is split into k approximately equal partitions and each in turn is used for testing and the remainder is used for training. Tenfold cross-validation is used in the relevant section. The dataset is divided randomly into 10 parts. Each part is held out in turn and the learning scheme is trained using the remaining nine-tenths. Then, its error rate is calculated on the holdout set. The learning procedure is executed a total of 10 times on different training sets. Finally, the 10 error estimates are averaged to yield an overall error estimate (Witten & Frank 2005).

ANN modeling using holdout method

In this study, a three-layer feedforward network with the sigmoid transfer function in the hidden layer and a linear transfer function in the output layer was used. The networks were trained by the backpropagation algorithm. To select an appropriate architecture, the guidelines advocated by Hecht-Nielson (1987) and Rogers & Dowla (1994) were used. Equations (13) and (14) present these guidelines, respectively:

$$N^H \leq N^I + 1 \tag{13}$$

$$N^H \leq \frac{N^{TR}}{N^I + 1} \tag{14}$$

where N^H is the number of hidden layer neurons, N^I is the number of inputs and N^{TR} is the number of training samples. To avoid overfitting of the ANN, an early stopping (Heskes 1997) criterion was used in the training process. The training process of the ANN was stopped when the performance of the ANN in the testing set started to decrease. To identify the relative importance of different phenomena/effective nondimensional parameters, several ANN models based on subjects mentioned earlier were developed and evaluated.

In the training process two factors were used to control the training algorithm's adjustment of the weights (learning rate coefficient and momentum factor). A large value of the learning rate may leads to instability in the training process. If the learning rate is too small, the network will learn at a very slow pace. The momentum factor has a smaller effect on learning speeds. However, it can affect training stability and promote faster learning for most networks. Higher values of the momentum factor can help the network escape from a local minimum.

In this study the best initial learning rate value and momentum factor were found to be 0.3 and 0.9, respectively. The training process was terminated if 96% of the samples successfully matched the expected output with the specified error tolerance (0.01).

ANN model considering flow-structure interaction

The way that a pipe is installed on the seabed and how flow affects the pipe are represented by the e/D, KC and Re parameters. These parameters show the vortex generation and motion behind the pipe (for more details see Sumer & Fredsoe (1997)). The effects of Re number on S/D has been assumed weak by other researchers (e.g. SF90), while in the

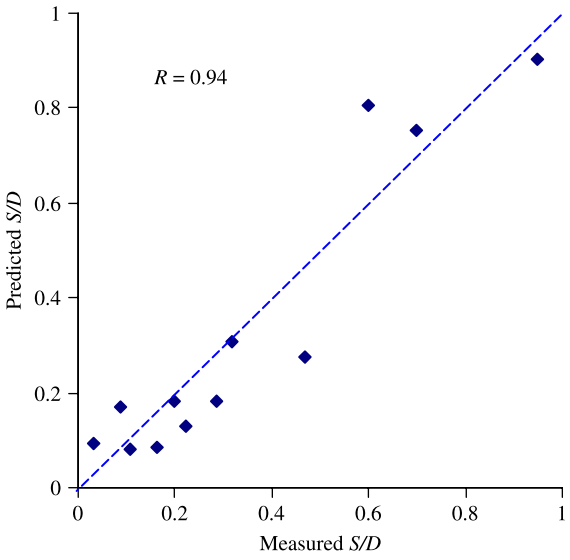

Figure 4 | Comparison between measured and predicted S/D by the M1 model ($2 \times 3 \times 1$) for testing data.

Table 6 | Error statistics of the predicted *S/D* by the ANN-based models and Sumer & Fredsoe (SF02) equation for testing data (holdout method)

Model	*e/D*	KC	Re	θ	Re_s	Re_0	*SI* (%)	Bias	*R*	Max. error (%)
SF02	✓	✓					37.82	0.03	0.92	629
M1	✓	✓					29.38	−0.015	0.94	193
M2	✓	✓	✓				25.27	−0.035	0.95	49
M3	✓	✓	✓	✓	✓		20.30	0.0002	0.97	50
M4	✓	✓	✓	✓	✓	✓	16.48	−0.01	0.98	45

previous section it was shown that there is a high correlation between *Re* and *S/D* parameters.

First an ANN model was developed with the *KC* and *e/D* as input parameters and *S/D* as the neuron in the output layer. The parameters used in the input layer are the governing parameters in the estimation of *S/D* in live bed conditions (Me06, SF90). The number of neurons in the hidden layer was varied from 2 to 5 to find the best network topology. Following Ustoorikar & Deo (2008) the criterion of selecting the best network topology was considered to be the minimum scatter index between the actual nondimensional scour depth and the corresponding predicted values obtained from the trained network. The best topology for the network with two neurons (*KC* and *e/D* parameters) in the input layer was $2 \times 3 \times 1$ (M1 model). The comparison between the measured and predicted nondimensional scour depths using the M1 model is shown in Figure 4. As can be seen, the predictions are scattered relative to the measurements, but they are not significantly biased. The performance of the developed ANN model is evaluated qualitatively in terms of the bias, scatter index, correlation coefficient and maximum error parameters. Table 6 shows the error statistics of the calculated scour depth for testing data. It can be seen that the M1 model slightly under-predicts (bias = -0.015) *S/D*. In addition, the scatter index for predicted *S/D* and the correlation coefficient between the predicted and measured *S/D* are 29.38% and 0.94, respectively.

Some of the observed error in the M1 model can be due to the omitting of other parameters which describe the flow–structure interaction, i.e. pipe Reynolds number. Therefore, an ANN model with three neurons in the input layer (*e/D*, *KC* and *Re*) was trained as the scour depth predictor. Networks with different numbers of neurons (from 2 to 7) in the hidden layer were examined and the best topology was found to be $3 \times 6 \times 1$ (M2 model). Figure 5 displays the comparison between measured and predicted *S/D* by the M2 model. The error statistics of the M2 model for testing data are presented in Table 6. It is seen that the M2 model underestimates *S/D* with the $SI = 25.27\%$ and $R = 0.95$. Comparison between the M1 and M2 statistical errors shows that the M2 model outperforms the M1 model. Therefore, it could be inferred that the *Re* parameter needs to be considered in the modeling of the wave-induced scour depth around a submarine pipeline.

ANN model considering different physical processes

In this section the effects of flow–seabed interaction, which was neglected by the other researchers, were considered in the development of the scour depth predictor model. The mutual effects of flow on the seabed were shown by the Shields parameter and sediment Reynolds number.

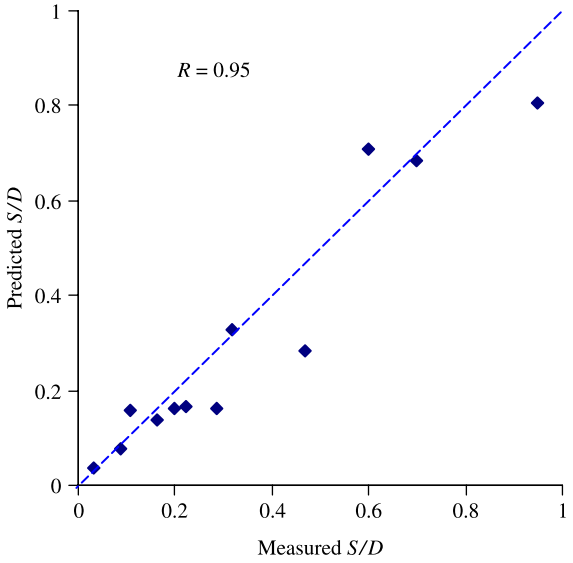

Figure 5 | Comparison between measured and predicted *S/D* by the M2 model ($3 \times 6 \times 1$) for testing data.

ANNs with five neurons in the input layer (e/D, KC, Re, θ and Re_s), different numbers of neuron (from 2 to 11) in the hidden layer and one neuron (S/D) in the output layer were trained to find the best topology. The network with $5 \times 9 \times 1$ topology was found to be the best network (M3 model). Figure 6 shows the comparison between the measured and predicted S/D using the M3 model. As can be seen the predictions are not biased. Table 6 shows the error statistics of the M3 model. The accuracy of the M3 model (bias = 0.0, $SI = 20.30\%$ and $R = 0.97$) is more than those of the M1 and M2 models. A comparison between the accuracies of the M1, M2 and M3 models indicates that including the θ and Re_s parameters in the model training increases the accuracy of the trained model.

Finally an ANN-based model was developed by considering all of the important processes occurring during development of the scour hole. Therefore, all the parameters presented on the right-hand side of Equation (10), which represent the mutual effects of flow on pipe and seabed, and boundary layer characteristics, were used to develop and train the model. The network consisted of six neurons in the input layer which were e/D, KC, Re, θ, Re_s and the boundary layer Reynolds number (Re_0). The best topology for this network was found to be $6 \times 13 \times 1$ (M4 model). Comparison between measured and predicted S/D by the M4 model is illustrated in Figure 7. As shown,

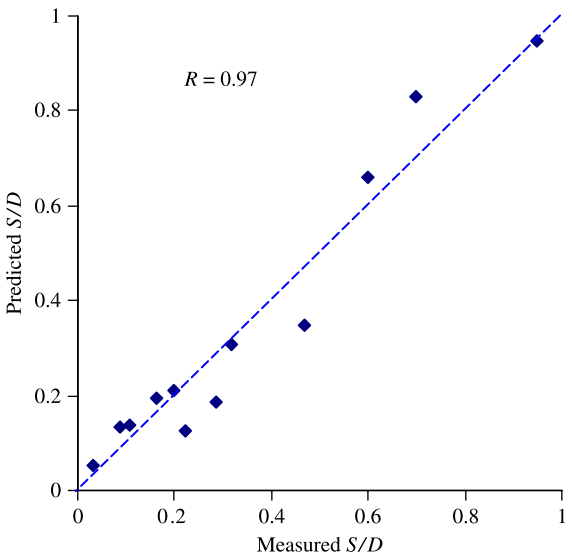

Figure 6 | Comparison between measured and predicted S/D by the M3 model ($5 \times 9 \times 1$) for testing data.

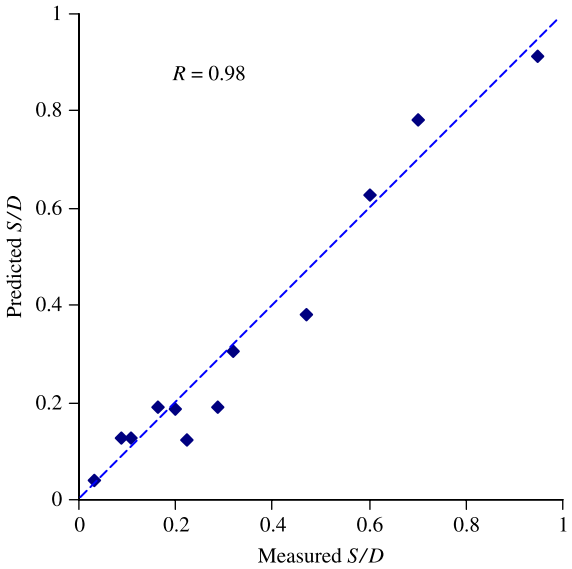

Figure 7 | Comparison between measured and predicted S/D by the M4 model ($6 \times 13 \times 1$) for testing data.

the M4 model performed quite well in prediction of the S/D. The error statistics of this model in predicting S/D are shown in Table 6. It can be seen that the M4 model marginally under-predicts (bias = −0.01) the nondimensional scour depth. The scatter index for predicted S/D and the correlation coefficient between the predicted and measured S/D are 16.48% and 0.98, respectively. Comparison of the accuracies of the ANN models shows that utilization of all the parameters introduced in Equation (10) improves the accuracy of the ANN model. This result is due to the fact that the scour phenomenon around a submarine pipeline is composed of different processes and the effects of all processes should be considered in the scour depth prediction.

To compare the performance of the developed ANN-based models with the existing empirical models, nondimensional scour depths were predicted by the SF02 equation (Figure 8). It is seen that this equation overpredicts the S/D parameter. Table 6 shows the error statistics of S/D calculated by the SF02 equation. The scatter index for the predicted S/D by this model is 37.82%. Although the SF02 and M1 inputs are the same, the accuracy of the M1 model, which is an ANN-based model, is higher than that of the SF02 model. This is in line with the results obtained by Kambekar & Deo (2003)

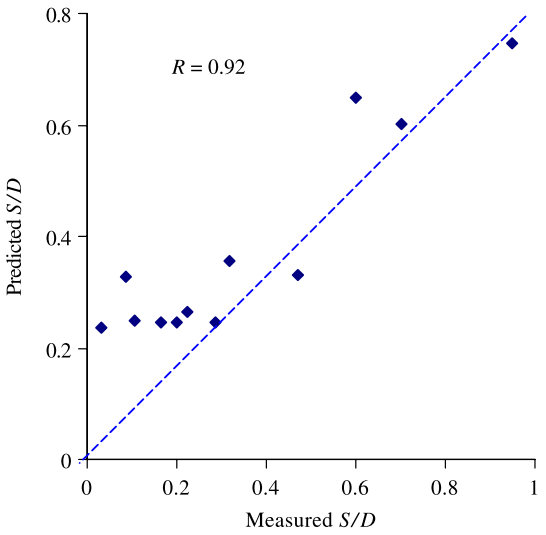

Figure 8 | Comparison between measured and predicted S/D by the SF02 model for testing data.

and Bateni *et al.* (2007*a*). They found that the ANN-based models outperform the empirical methods in the prediction of scour depth around piles.

ANN modeling using tenfold cross-validation

In this section the M1, M2, M3 and M4 models were trained and evaluated using the tenfold cross-validation method. Therefore the dataset was equally divided into 10 parts. The training and testing were carried out 10 times for each model using one distinct set for testing and the remaining nine for training. Finally, there were 10 testing sets with every record appearing in the testing sets once. Table 7 presents the average errors over the 10 testing sets. As can be seen, the M4 model which contains all related non-dimensional parameters as input parameters outperforms the other models. Comparison between Tables 6 and 7 indicates that using the holdout method results in lower error values. This shows that application of the holdout method may lead to unrealistic errors. Table 7 also shows the error statistics of the SF02 equation for all datasets. Results of M1 and SF02 models show that utilization of ANN-based models leads to lower error statistics (especially maximum error). As can be seen, use of important nondimensional parameters in the ANN model increases the accuracy in the prediction of S/D. This results in 11.65% reduction in the average error and 112% reduction in the maximum error.

To see if the best trained network (M4 model) behaves as expected from the physical understanding, a parametric study with varying input variables was carried out. First, variation of S/D against KC parameter is studied. To do so the e/D, Re, θ, Re_s and Re_0 were considered to be 0, 3000, 0.65, 6 and 10,000, respectively, and the KC parameter was varied from 2 to 92 (Figure 9). As expected, the scour depth increases as the KC number increases. Figure 10 displays the variation of S/D against e/D. As can be seen, the scour depth decreases as the gap to diameter ratio is increased which is physically accepted. Both these results are in line with the previous understanding of the scour process (SF02).

The limitations of ANN models need to be mentioned as well. Several studies have reported that the ANN model performs well when it is faced with problems that fall within the domain of inputs that were used for training. Therefore, similar to empirical models ANN models cannot be used for extrapolation. One way around this problem is to use the widest limits of examples during training. In this study, to ensure that the developed ANN models do not have to extrapolate, they were trained based on the widest limits of nondimensional parameters; hence they are applicable both for laboratory scale and prototype conditions. This is the main ability and advantage of the

Table 7 | Error statistics of the predicted S/D by the ANN-based models and Sumer & Fredsoe (SF02) equation using tenfold cross-validation method

Model	e/D	KC	Re	θ	Re_s	Re_0	SI (%)	Bias	R	Max. error (%)
SF02	✓	✓					39.26	0.036	0.90	1,071
M1	✓	✓					35.43	−0.003	0.86	198
M2	✓	✓	✓				33.47	0.004	0.90	127
M3	✓	✓	✓	✓	✓		27.04	0.012	0.94	109
M4	✓	✓	✓	✓	✓	✓	23.78	0.009	0.95	86

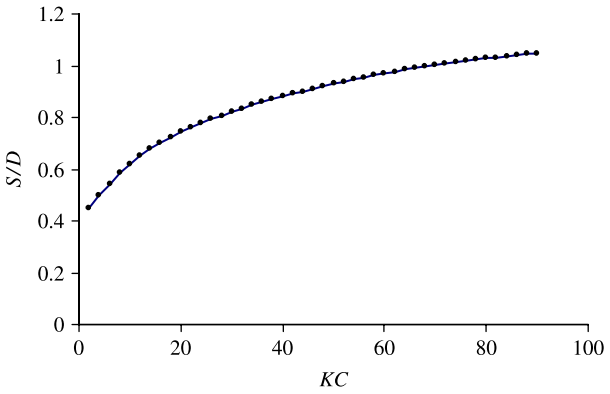

Figure 9 | Variation of the S/D parameter against the KC number for $e/D = 0$, $Re = 3{,}000$, $\theta = 0.65$, $Re_s = 6$ and $Re_0 = 10{,}000$ using the M4 model.

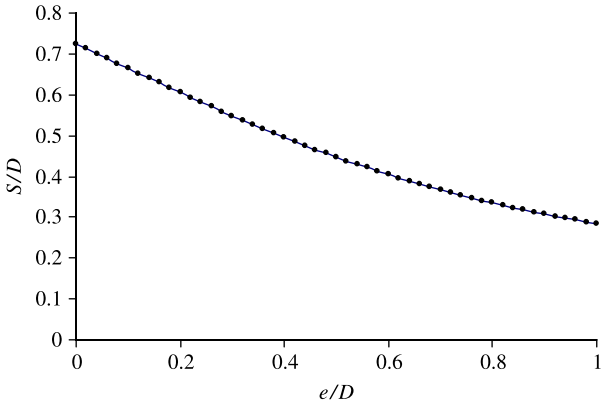

Figure 10 | Variation of the S/D parameter against the e/D parameter for $KC = 20$, $Re = 3{,}000$, $\theta = 0.65$, $Re_s = 6$ and $Re_0 = 10{,}000$ using the M4 model.

developed models in comparison with some other models developed based on dimensional parameters. It should also be mentioned that employing the original (dimensional) data rather than the nondimensional data in the training process may lead to better results in the scour depth prediction (e.g. Kambekar & Deo 2003; Bateni *et al.* 2007*a*). However, the model trained with laboratory dimensional data may not be directly applicable in the field.

SUMMARY AND CONCLUSIONS

In this study the equilibrium wave-induced scour depth around submarine pipelines was studied using the experimental dataset of SF90, Pe01 and Me06. The nondimensional parameters were considered as the model's inputs and outputs to be applicable in the field. First, effective nondimensional parameters were investigated by calculating the correlation coefficients between independent nondimensional parameters and equilibrium scour depth. Analyses indicate that, in addition to the KC and e/D parameters, other nondimensional parameters such as Re have significant correlation with S/D. The Sumer & Fredsoe (2002) equation was examined using different experimental data. It was found that this equation is relatively accurate in the cases with no initial gap between pipe and seabed.

To consider all effective parameters in the development of the scour predictor model, the Artificial Neural Network technique was used. To develop an error estimate of the models, the holdout and tenfold cross-validation methods were used. Different models based on different input parameters were trained and tested. In the training of each model the best topology was found by trial and error. Results showed that the model including the e/D, KC, Re, θ, Re_s and Re_0 parameters in input layers is the most accurate one. The estimated average error of this model in the prediction of S/D based on tenfold cross-validation is 23.78% while the error of the SF02 empirical model is 39.26%. In comparison with the SF02 equation, the ANN-based models result in lower maximum error and average error in the prediction of S/D.

One of the limitations of this study is due to the application of the ANN. One disadvantage of ANN models is that the optimum neural network parameters as well as the optimum network geometry (i.e. the number of hidden layers and the number of nodes per hidden layer) are problem-dependent and generally have to be found using a trial-and-error approach (Maier & Dandy 1995). In addition the rules of operation in ANN models are completely unknown and it is not possible to convert the neural structure into known model structures. The other limitation of this study is the lack of extensive data. Further research should be aimed at obtaining more physical insight from soft computing tools such as ANNs using extensive data.

ACKNOWLEDGEMENTS

We are grateful to three anonymous reviewers for their helpful comments. In addition, the first two authors expresses special thanks to Javad Mahjoubi and Mohammad Ayoubloo for their great efforts.

REFERENCES

Azamathullau, H. Md., Deo, M. C. & Deolalikar, P. B. 2008 Alternative neural networks to estimate the scour below spillways. *Adv. Eng. Softw.* **39** (8), 689–698.

Bateni, S. M. & Jeng, D.-S. 2007 Estimation of pile group scour using adaptive neuro-fuzzy approach. *Ocean Eng.* **34** (8–9), 1344–1354.

Bateni, S. M., Borghei, S. M. & Jeng, D.-S. 2007 Neural network and neuro-fuzzy assessments for scour depth around bridge piers. *Eng. Appl. Artificial Intell.* **20** (3), 401–414.

Bateni, S. M., Jeng, D.-S. & Melville, B. W. 2007 Bayesian neural networks for prediction of equilibrium and time-dependent scour depth around bridge piers. *Adv. Eng. Softw.* **38** (2), 102–111.

Cevik, E. & Yuksel, Y. 1999 Scour under submarine pipelines in waves in shoaling conditions. *J. Waterway Port Coastal Ocean Eng. ASCE* **125** (1), 9–19.

Chau, K. W. 2006 A review on the integration of artificial intelligence into coastal modeling. *J. Environ. Manage.* **80** (1), 47–57.

Chau, K. W. & Muttil, N. 2007 Data mining and multivariate statistical analysis to ecological system in coastal waters. *J. Hydroinf.* **9** (4), 305–317.

Deo, M. C., Jha, A., Chaphekar, A. S. & Ravikant, K. 2001 Neural networks for wave forecasting. *Ocean Eng.* **28** (7), 889–898.

Geman, S., Bienenstock, E. & Doursat, R. 1992 Neural networks and the bias variance dilemma. *Neural Comput.* **4** (1), 1–58.

Hecht-Nielson, R. 1987 Kolmogorov's mapping neural network existence theorem. In: *Proceedings of the First IEEE International Joint Conference on Neural Networks*, *Vol. 3*. IEEE, New York, pp. 11–14.

Heskes, T. 1997 Balancing between bagging and bumping. *Adv. Neural Inf. Process. Syst.* **9**, 466–472.

Jonsson, I. G. 1967 Wave boundary layers and friction factors. In: *Proceedings of the 10th International Conference on Coastal Engineering, Tokyo, Japan*, pp. 127–148 ASCE, New York.

Kambekar, A. R. & Deo, M. C. 2003 Estimation of pile group scour using neural networks. *Appl. Ocean Res.* **25** (4), 225–234.

Kazeminezhad, M. H., Etemad-Shahidi, A. & Mousavi, S. J. 2005 Application of fuzzy inference system in the prediction of wave parameters. *Ocean Eng.* **32** (14–15), 1709–1725.

Kerh, T. & Yee, Y. C. 2000 Analysis of a deformed three-dimensional culvert structure using neural networks. *Adv. Eng. Softw.* **31** (5), 367–375.

Liang, D. & Cheng, L. 2005 Numerical model for wave-induced scour below a submarine pipeline. *J. Waterway Port Coast. Ocean Eng. ASCE* **131** (5), 193–202.

Liriano, S. L. & Day, R. A. 2001 Prediction of scour depth at culvert outlets using neural networks. *J. Hydroinf.* **3** (4), 231–238.

Lucassen, R. J. 1984 *Scour Underneath Submarine Pipelines*. MATs Report PL-4 2A. Marine Technical Research, The Netherlands.

Mahjoobi, J., Etemad-Shahidi, A. & Kazeminezhad, M. H. 2008 Hindcasting of wave parameters using different soft computing methods. *Appl. Ocean Res.* **30** (1), 28–36.

Maier, H. R. & Dandy, G. C. 1995 *Comparison of the Box–Jenkins Procedure with Artificial Neural Network Methods for Univariate Time Series Modeling*. Research Report R127. Department of Civil and Environmental Engineering, University of Adelaide, Australia.

Manache, G. & Melching, C. S. 2008 Identification of reliable regression-and correlation-based sensitivity measures for importance ranking of water-quality model parameters. *Environ. Modell. Softw.* **23** (5), 549–562.

Mao, Y. 1986 *The Interaction Between a Pipeline and an Erodible Bed*. PhD Thesis, Institute of Hydrodynamics and Hydraulic Engineering, Technical University of Denmark, Lyngby, Denmark.

McCulloch, W. & Pitts, W. 1943 A logical calculus of the ideas immanent in nervous activity. *Bull. Math. Biophys.* **7**, 115–133.

Mousavi, M. E., Yeganeh–Bakhtiary, A. & Enshaei, N. 2006 The equivalent depth of wave-induced scour around offshore pipelines. In: *Proceedings of the 25th International Conference on Offshore Mechanics and Arctic Engineering, Hamburg, Germany*. ASME No. 92049.

Muttil, N. & Chau, K. W. 2006 Neural network and genetic programming for modeling coastal algal blooms. *Int. J. Environ. Pollut.* **28** (3–4), 223–238.

Pu, Q., Li, K. & Gao, F. P. 2001 Scour of the seabed under a pipeline in oscillating flow. *China Ocean Eng.* **15** (1), 129–137.

Rogers, L. L. & Dowla, F. U. 1994 Optimization of groundwater remediation using artificial neural networks with parallel solute transport modeling. *Water Resour. Res.* **30** (2), 457–481.

Ruessink, B. G. 2005 Calibration of nearshore process models–application of a hybrid genetic algorithm. *J. Hydroinf.* **7** (2), 135–149.

Soulsby, R. 1997 *Dynamics of Marine Sands, A Manual For Practical Applications*. Thomas Telford, London.

Stone, M. 1974 Cross validation choice and assessment of statistical predictions. *J. R. Stat. Soc. B* **36**, 111–147.

Sumer, B. M. & Fredsoe, J. 1990 Scour below pipelines in waves. *J. Waterway Port Coast. Ocean Eng. ASCE* **116** (3), 307–323.

Sumer, B. M. & Fredsoe, J. 1997 *Hydrodynamics Around Cylindrical Structures*. World Scientific, Singapore.

Sumer, B. M. & Fredsoe, J. 2002 *The Mechanics of Scour in the Marine Environment*. World Scientific, Singapore.

Sumer, B. M., Jensen, B. L. & Fredsoe, J. 1991 Effect of a plane boundary on oscillatory flow around a circular cylinder. *J. Fluid Mech.* **225**, 271–300.

Sumer, B. M., Truelsen, C., Sichmann, T. & Fredsoe, J. 2001 Onset of scour below pipelines and self-burial. *Coast. Eng.* **42** (4), 313–335.

Ustoorikar, K. & Deo, M. C. 2008 Filling up gaps in wave data with genetic programming. *Mar. Struct.* **21** (2–3), 177–195.

Van Rijn, L. C. 1993 *Principles of Sediment Transport in Rivers, Estuaries and Coastal Seas*. Amsterdam Aqua Publication, Amsterdam, The Netherlands.

Witten, I. H. & Frank, E. 2005 *Data Mining: Practical Machine Learning Tools and Techniques*. Morgan Kaufmann, San Francisco, CA.

Zhang, Z., Li, C. W., Li, Y. S. & Qi, Y. 2006 Incorporation of artificial neural networks and data assimilation techniques into a third-generation wind-wave model for wave forecasting. *J. Hydroinf.* **8** (1), 65–76.

Zhao, Z. & Fernando, H. J. S. 2007 Numerical simulation of scour around pipelines using an Euler-Euler coupled two-phase model. *Environ. Fluid Mech.* **7** (2), 121–142.

First received 12 May 2008; accepted in revised form 27 September 2008. Available online September 2009